

On the Thermal Contact Resistance Effects in Aluminum-Galvanized Steel Wires OPGW Submitted to a Short-Circuit Test

Sergio Colle¹ and Marcelo de Araújo Andrade²

¹Department of Mechanical Engineering / Federal University of Santa Catarina
Florianópolis, Santa Catarina, Brazil

+55-48-2342161 / 2340408 · colle@emc.ufsc.br

²Pirelli Telecomunicações Cabos e Sistemas do Brasil S.A.
Sorocaba – São Paulo – Brazil

+55-15-32359209 · marcelo.andrade@pirelli.com.br

Abstract

The heat transfer during the short-circuit test of an OPGW manufactured with aluminum tube and galvanized wires, has been investigated by many authors. In spite of the fact the temperature gradient in the aluminum wires can be neglected, it is shown in this paper the temperature gradient have a significant effect on the cooling of the aluminum tube. The present work reports the experimental results and the predicted temperature results obtained from a general analytical solution of the heat conduction equations of the tube and the wires, for a cable Pirelli OPGW-SM-16.4 48 FO (10.2mm O.D. aluminum tube – 13 galvanized wires ϕ 3.12mm). The analytical solution is expressed in terms of the thermophysical properties of the materials of the tube and the wire, as well as the geometrical design parameters of the cable. The thermal contact resistance between the tube and the wires is also taken into account.

Keywords: Short-circuit test; OPGW; unsteady heat-transfer.

1. Introduction

The short-circuit current carrying capacity of an OPGW conductor is thermally limited by maximum temperatures to prevent annealing of the aluminum wires and bird-caging of the conductor. The thermal response of the conductor is dependent of the product $I^2 \Delta t_c$, of the effective current intensity and the time interval of the short-circuit. The maximum temperatures achieved by the aluminum tube and the strand wires depend not only on this term, but also depend on the thermal properties of the materials, the electric resistance of the conductor components, the geometry of the conductor, as well as the contact thermal resistance between the strand wires and the aluminum tube. Figure 1 illustrates a picture of the aluminum tube of the OPGW analyzed here. The discontinuous



Figure 1. Aluminum tube of the OPGW

strips seen in the surface of the tube are due to the effective mechanical contact between the strand wires and the tube.

In the case of OPGW made of galvanized steel wires, most part of the electric current is oriented to the aluminum tube. Therefore the aluminum tube achieves the maximum temperature peak while the strand wires heat up slowly. The temperature difference between the tube and the wires, as well as the fact that the aluminum linear thermal coefficient expansion be greater than the linear thermal expansion coefficient of the steel wires, lead to thermal stresses in the aluminum tube. These induced stresses may cause the tube creeping and therefore, the optical fibers damage. The fibers usually reach their highest temperature much later than the aluminum tube reach its highest temperature, which means that the equivalent radial thermal conductivity of the packed fibers is much smaller than the thermal conductivity of the aluminum. Therefore as a first approximation, the heat conduction on the fibers can be neglected, in comparison to the heat conduction in the metallic components of the conductor.

In designing an OPGW, one should take into account not only the thermal and mechanical properties of the materials of the OPGW components but also the size and the shape of its components. The present analysis focuses the study of the heat transfer of OPGW submitted to a short-circuit current. The analytical solution obtained is expressed in terms of the relevant geometrical dimensions of the aluminum tube and the strand wire. Dimensionless numbers are obtained which can be useful for OPGW design.

2. Governing Equations

By neglecting the temperature gradient in the aluminum tube and the heat transfer to the fibers, the energy balance in the tube (see Figures 2(a) and (b)) can be expressed as,

$$\rho_i c_i \pi (R_o^2 - R_i^2) L \frac{dT_i}{dt} = I_i^2 R_i - N_a L_o 2r_a k_a \int_0^{\phi_o} \left. \frac{\partial T_a}{\partial r} \right|_{r_a} d\phi \quad (1)$$

where L_o is the length of the effective thermal contact surface strip of width $2e_a$, N_a is the number of wires of the strand, k_a is the thermal conductivity of the wire material, r_a is the wire radius, R_o and R_i are the inner and outer radii of the aluminum tube, respectively.

Equation (1) can be reduced to a non-dimensional equation as follows,

$$\alpha \frac{d\theta_i}{d\tau} = p_i - \frac{2}{\pi} F_{oa} N_a \sqrt{1 + \lambda_o^2} \int_0^{\phi_o} \phi(\phi, \tau) d\phi \quad (2)$$

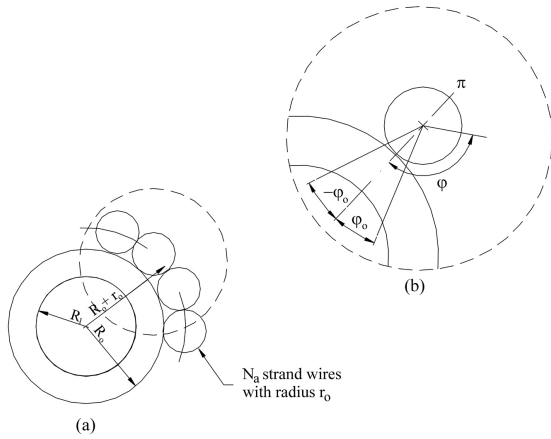


Figure 2. Cross section geometry of the OPGW

where $\theta = \frac{T - T_o}{T_o}$, $\eta = r/r_a$, $\phi(\tau) = \frac{\partial \theta_a}{\partial \eta}(1, \varphi, \tau)$, ϕ is the dimensionless heat flux, $\tau = t/\Delta t_c$, T_o is the initial temperatures, Δt_c is the short-circuit duration time, $\alpha = \rho_a c_a \pi (R_o^2 - R_i^2) / \rho_a c_a \pi r_a^2$, ρ is the specific mass, c is the specific heat, $F_{oa} = k_a \Delta t_c / \rho_a c_a r_a^2$ is the Fourier number of the wire, $p_i = (I^2 \Delta t_c) R_{20i} \lambda_r^2 f_i f_a^2 / (f_i + \lambda_r f_a)^2 \rho_a c_a \pi r_a^2 L T_o$, $\lambda_r = \frac{R_{20a}}{N_a R_{20i}} = \left(\frac{\rho_{20a}}{\rho_{20i}} \right) (R_o^2 - R_i^2) \frac{\sqrt{1 + \lambda_a^2}}{N_a r_a^2}$, $\lambda_o = \frac{2\pi R_o}{L}$, f_i and f_a are the electrical resistance temperature-depended functions of the aluminum and steel, respectively, R_{20} is the electrical resistance at 20°C and ρ_{20} is the electrical resistivity at 20°C.

The energy balance in the wire is governed by the following equation

$$k_a \frac{1}{r} \frac{\partial}{\partial r} \left(r \frac{\partial T_a}{\partial r} \right) + \frac{I_a^2 R_a}{\pi r_a^2 L_a} = \rho_a c_a \frac{\partial T_a}{\partial t} \quad (3)$$

where I_a is the current intensity in the wire. The dimensionless form of equation (3) is given by,

$$\frac{1}{\eta} \frac{\partial}{\partial \eta} \left(\eta \frac{\partial \theta_a}{\partial \eta} \right) + \frac{p_a}{F_{oa}} = \frac{1}{F_{oa}} \frac{\partial \theta_a}{\partial \tau} \quad (4)$$

where $p_a = (I^2 \Delta t_c) R_{20a} f_a f_i^2 / (f_i + \lambda_r f_a)^2 \rho_a c_a \pi r_a^2 L_a T_o N_a^2$.

The boundary and interface conditions for equation (2) and (4) are given by

$$\frac{\partial \theta_a}{\partial \eta}(1, \varphi, \tau) = \phi(\varphi, \tau) \text{ for } -\varphi_0 \leq \varphi \leq \varphi_0 ; \tau > 0 \quad (5)$$

and

$$\frac{\partial \theta_a}{\partial \eta}(1, \varphi, \tau) = 0 \text{ for } |\varphi| > \varphi_0 \quad (6)$$

The initial conditions are,

$$\theta_i(0) = \theta_a(\eta, \varphi, 0) = 0 \quad (7)$$

Equations (2) and (3) are non-linear because the heat source parameters p_i and p_a are temperature-dependent. In order to simplify the solution of equations (2) and (3) it is assumed that p_i and p_a are constant and evaluated at some temperature T_r , which is determined by a numerical scheme.

The thermal contact resistance in the interface between the wires and the tube is expressed by the equation,

$$k_a \frac{\partial T_a}{\partial r} \Big|_{r_a} = -h(T_a(r_a, \varphi, t) - T_i(t)) \quad (8)$$

or in the dimensionless form,

$$\phi(\tau, \varphi) = -B_i(\theta_a(1, \varphi, \tau) - \theta_i(\tau)) \quad (9)$$

where h is the heat transfer coefficient by convection and $B_i = h r_a / k_a$ is the Biot number referred to the wire diameter. The boundary condition given by equation (9) is not assumed to hold for each value of the angle φ . In order to simplify the analytical solutions for θ_a and θ_i , condition (9) is expressed in terms of the following integral suggested by the Galerkin method [1],

$$\int_0^{\varphi_0} [\phi(\varphi, \tau) + B_i(\theta_a(1, \varphi, \tau) - \theta_i(\tau))] \cos n\varphi d\varphi = 0 \quad (10)$$

In the present analysis only the integral for $n = 0$ is considered. Furthermore, since the angle φ_0 is considered to be small, $\phi(\varphi, \tau)$ can be assumed to be independent of φ and therefore,

$$\int_0^{\varphi_0} \phi(\varphi, \tau) d\varphi = \phi(\tau) \varphi_0 \quad (11)$$

Instead of considering the value of θ_a for each value of the angle φ in the interval $[0, \varphi_0]$, $\theta_a(1, \varphi, \tau)$ is replaced by its average in the interval $[0, \varphi_0]$ given by

$$\bar{\theta}_a(\tau) = \frac{1}{\varphi_0} \int_0^{\varphi_0} \theta_a(1, \varphi, \tau) d\varphi \quad (12)$$

By replacing $\theta_a(\tau)$ and $\phi(\tau)$ from equations (11) and (12) into equation (10), the following equations is obtained,

$$\phi(\tau) = -B_i(\bar{\theta}_a(\tau) - \theta_i(\tau)) \quad (13)$$

Equation (4) with the boundary conditions given by equations (5), (6) and (7) can be solved by the Green function method as described in [1,2,3]. For the above equations, the solution of equation (4) can be expressed by

$$\begin{aligned} \theta_a(1, \varphi, \tau) = & p_a \tau + \\ & + F_{oa} \int_0^{\tau} \left[\frac{2}{\pi} \varphi_0 + \frac{2}{\pi} \varphi_0 \sum_{m=1}^{\infty} e^{-\beta_m^2 F_{oa}(\tau-\tau')} \right. \\ & \left. + \frac{4}{\pi} \sum_{m,n=1}^{\infty} e^{-\beta_m^2 F_{oa}(\tau-\tau')} \cos n\varphi \frac{\text{senn}\varphi_0}{n} \frac{1}{(1-n^2/\beta_m^2)} \right] \phi(\tau') d\tau' \end{aligned} \quad (14)$$

or in terms of $\bar{\theta}_a(\tau)$ by

$$\bar{\theta}_a(\tau) = p_a \tau + \frac{2\varphi_0 F_{oa}}{\pi} \int_0^\tau \left[1 + \sum_{m=1}^{\infty} e^{-\beta_m^2 F_{oa}(\tau-\tau')} \right. \\ \left. + \frac{2}{\varphi_0^2} \sum_{m,n=1}^{\infty} \frac{\text{sen}^2 n \varphi_0}{n^2} \frac{e^{-\beta_m^2 F_{oa}(\tau-\tau')}}{(1-n^2/\beta_m^2)} \right] \phi(\tau') d\tau' \quad (15)$$

where β_n^m is the m-th root of the derivative of the Bessel function of the first kind of order $n=0,1,2, \dots$. $J'_n(\beta_m^n) = 0$; $m=1,2, \dots$

The solution for $\theta_i(\tau)$ and $\theta_a(1, \varphi, \tau)$ can be obtained by the method of Laplace transform. The inversion of the transformed identities is performed by the residues theorem of the calculus of functions of complex variables []. The solution for $\phi(\tau)$ can be expressed as follows

$$\phi^<(\tau) = \frac{\pi(p_i - \alpha p_a)}{2F_{oa}\varphi_0} \left(\frac{1}{H(0)} + \sum_{k=1}^{\infty} \frac{e^{p_k F_{oa}\tau}}{p_k H'(p_k)} \right) \quad \text{for } \tau \leq 1 \quad (16)$$

$$\phi^>(\tau) = \frac{\pi(p_i - \alpha p_a)}{2F_{oa}\varphi_0} \sum_{k=1}^{\infty} \frac{(e^{p_k F_{oa}(\tau-1)} - e^{p_k F_{oa}\tau})}{p_k H'(p_k)} \quad \text{for } \tau > 1 \quad (17)$$

where

$$H(p) = \frac{\pi\alpha p}{2\varphi_0 B_i} + \alpha + N_a \sqrt{1 + \lambda_o^2} + \alpha p \sum_{m=1}^{\infty} \frac{1}{(p + \beta_m^2)} \\ + \frac{2\alpha p}{\varphi_0^2} \sum_{m,n=1}^{\infty} \frac{\text{sen}^2 n \varphi_0}{n^2} \frac{1}{(1-n^2/\beta_m^2)} \frac{1}{(p + \beta_m^2)} \quad (18)$$

and p_k is the root of $H(p) = 0$.

The solution for $\theta_i(\tau)$ is given by

$$\theta_i^<(\tau) = C_i \tau - \frac{(p_i - \alpha p_a)}{\alpha F_{oa}} N_a \sqrt{1 + \lambda_o^2} \sum_{k=1}^{\infty} \frac{(e^{p_k F_{oa}\tau} - 1)}{p_k^2 H'(p_k)} \quad (19)$$

for $\tau \leq 1$

where

$$C_i = \frac{p_i + N_a \sqrt{1 + \lambda_o^2} p_a}{\alpha + N_a \sqrt{1 + \lambda_o^2}} \quad (20)$$

and

$$\theta_i^>(\tau) = C_i + \frac{(p_i - \alpha p_a)}{\alpha F_{oa}} N_a \sqrt{1 + \lambda_o^2} \sum_{k=1}^{\infty} \frac{(e^{p_k F_{oa}(\tau-1)} - e^{p_k F_{oa}\tau})}{p_k^2 H'(p_k)} \quad (21)$$

for $\tau > 1$.

The solution for the temperature at the center of the wire ($\eta = 0$) is given by

$$\theta_{ao}^<(\tau) = \theta_a(0, \varphi, \tau) = C_i \tau + \frac{(p_i - \alpha p_a)}{F_{oa}} \left[\sum_{k=1}^{\infty} \frac{(e^{p_k F_{oa}\tau} - 1)}{p_k^2 H'(p_k)} \right. \\ \left. + \frac{1}{\alpha + N_a \sqrt{1 + \lambda_o^2}} \sum_{m=1}^{\infty} \frac{(1 - e^{-\beta_m^2 F_{oa}\tau})}{\beta_m^2 J_o(\beta_m^0)} \right. \\ \left. + \sum_{m,k=1}^{\infty} \frac{(e^{p_k F_{oa}\tau} - e^{-\beta_m^2 F_{oa}\tau})}{J_o(\beta_m^0) (p_k + \beta_m^2) p_k H'(p_k)} \right] \quad (22)$$

for $\tau \leq 1$

and

$$\theta_{ao}^>(\tau) = C_i + \frac{(p_i - \alpha p_a)}{F_{oa}} \left\{ \sum_{k=1}^{\infty} \frac{(e^{p_k F_{oa}\tau} - e^{p_k F_{oa}(\tau-1)})}{p_k^2 H'(p_k)} \right. \\ \left. + \frac{1}{(\alpha + N_a \sqrt{1 + \lambda_o^2})} \sum_{m=1}^{\infty} \frac{(e^{-\beta_m^2 F_{oa}(\tau-1)} - e^{-\beta_m^2 F_{oa}\tau})}{\beta_m^2 J_o(\beta_m^0)} \right. \\ \left. + \sum_{m,k=1}^{\infty} \left[\frac{(e^{p_k F_{oa}\tau} - e^{p_k F_{oa}(\tau-1)})}{J_o(\beta_m^0) (p_k + \beta_m^2) p_k H'(p_k)} \right. \right. \\ \left. \left. - \frac{(e^{-\beta_m^2 F_{oa}\tau} - e^{-\beta_m^2 F_{oa}(\tau-1)})}{J_o(\beta_m^0) (p_k + \beta_m^2) p_k H'(p_k)} \right] \right\} \quad (23)$$

for $\tau > 1$.

The average temperature θ_{am} over the cross section of the wire is expressed by

$$\theta_{am}^<(\tau) = C_i \tau + \frac{(p_i - \alpha p_a)}{F_{oa}} \sum_{k=1}^{\infty} \frac{(e^{p_k F_{oa}\tau} - 1)}{p_k^2 H'(p_k)} \quad (24)$$

for $\tau \leq 1$ and

$$\theta_{am}^>(\tau) = C_i + \frac{(p_i - \alpha p_a)}{F_{oa}} \sum_{k=1}^{\infty} \frac{(e^{p_k F_{oa}(\tau-1)} - e^{p_k F_{oa}\tau})}{p_k^2 H'(p_k)} \quad (25)$$

for $\tau > 1$.

By inspection of equations (19)-(25) it is seen that for large values of time, $\theta_i^<(\tau)$, $\theta_{ao}^>(\tau)$, and $\theta_{am}^>(\tau)$ tend asymptotically to the value given by C_i as expressed by equation (20). It can be shown that C_i is proportional to the adiabatic equilibrium temperature of the conductor, as expected.

3. Discussion of Results

3.1 Predicted Results

The analytical solution obtained here in terms of the temperature of the tube, is compared with the respective solution of the present problem, by neglecting the temperature gradients in the wires, which means that only the thermal capacitances of the tube and the wires are taken into account. The results are shown in Figure (3) for different values of the thermal contact resistance parameter B_{ic} , where $B_{ic} = 2F_{oa} B_i \varphi_0 / \pi = h \Delta t_c e_a / \pi \rho_a c_a r_a^2$. This figure shows that for relatively small values of the parameter B_{ic} , the temperature distributions obtained from the thermal capacitance model (MCT)

are in agreement with the respective temperature distributions obtained from the present model (MGA). The smaller the values of B_{ic} , the smaller the effects of the temperature gradient in the wires on the temperature distributions of both, the tube and the wire. Figure (4) shows the effect of the thermal conductivity of the wire material on the temperature distributions, for $B_{ic} = 1.0$ and $\varphi_o = \pi/20$. The cases corresponding to aluminum wires and the fictitious case corresponding to the thermal conductivity coefficient equal to $1000\text{W/m}^\circ\text{C}$ are illustrated. The curve corresponding to model MCT is the limit-case for which the thermal conductivity is infinite.

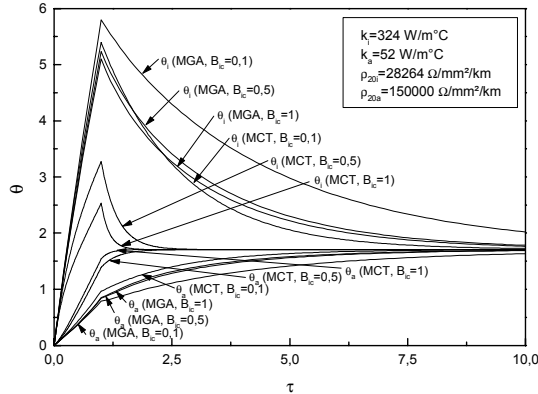


Figure 3. Temperature distributions of the tube and the wires, for several values of B_{ic} , for the present model (MGA) and for the thermal capacitance model (MCT)

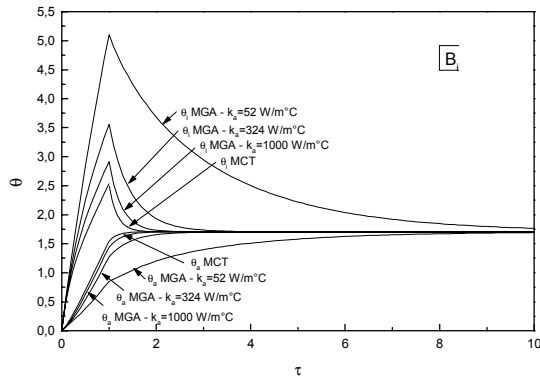


Figure 4. Comparison of results from models MGA and MCT for different values of the thermal conductivity of the wire, for $\varphi_o = \pi/20$ and $B_{ic} = 1$.

Figure (5) illustrates the effect of the contact angle φ_o on the maximum temperature achieved in the tube, as a function of parameter B_{ic} . As is seen in this figure, the maximum temperature depends also of the size of the angle φ_o , for almost all values of B_{ic} . An important design parameter derived in the present analysis is the factor $p_i - \alpha p_a$, which appears in the analytical solutions

for θ_i , θ_a and ϕ . This parameter measures the extent the current unbalance in the tube and the wires may increase or decrease the heat flux in the interface. The smaller the value of $p_i - \alpha p_a$, the smaller the maximum value achieved by the heat flux, and therefore the smaller the maximum temperature achieved in the tube.

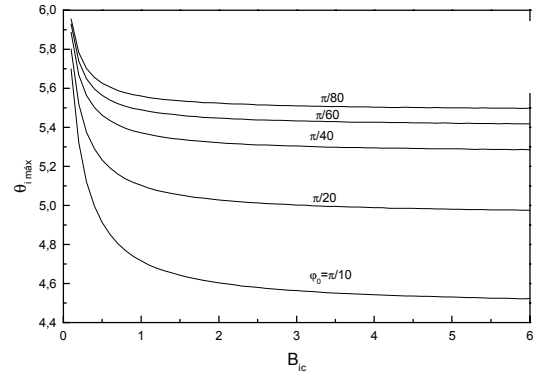


Figure 5. Maximum temperatures achieved in the tube for different contact angles, as a function of the parameter B_{ic}

The characteristic function $H(p)$ is plotted in Figure (6) as a function of p . Some roots of $H(p) = 0$ are shown in Table 1.

Here, $S_o = \frac{1}{H(0)} + \sum_{k=1}^N \frac{1}{p_k H'(p_k)}$, is the sum contained in the brackets of the second term on the right of equation (16), for $\tau = 0$. This sum should be zero, since the heat flux at $\tau = 0$ vanishes.

Table 1. Roots of $H(p) = 0$ for $B_{ic} = 1$ and 2

k	p_k	$H'(p_k)$	S_o
$B_{ic} = 1$			
1	-0.4625	40.86769	0.00093
2	-3.65313	468.3826	0.00035
3	-9.63242	1102.57	0.00025
4	-14.7664	6392.291	0.00024
5	-18.0031	1711.951	0.00021
6	-28.365	99139.12	0.00021
7	-28.8993	1764.909	0.00019
8	-41.5276	3993.86	0.00018
$B_{ic} = 2$			
1	-0.7375	26.19427	0.00207
2	-3.87344	151.8637	0.00037
3	-9.87578	355.1049	0.00009
4	-14.8284	2167.307	0.00006
5	-18.3047	516.2231	-0.00005
6	-28.3694	103783.5	-0.00005
7	-29.3715	527.2273	-0.00011
8	-41.8131	1303.227	-0.00013
9	-45.3877	1793.717	-0.00014
10	-49.4083	4344.281	-0.00015
11	-57.0022	1381.912	-0.00016
12	-64.6314	2905.68	-0.00017
13	-73.0317	20421.91	-0.00017
14	-74.5254	1211.448	-0.00018

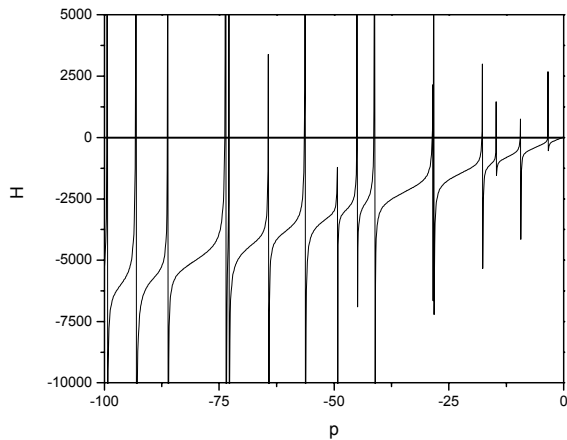


Figure 6. Typical plot of $H(p)$

3.2 Experimental Results

The cable OPGW Pirelli SM 14.6 48FO was tested in the test facility of the laboratory of CEPEL (Research Center of ELETROBRAS) in Rio de Janeiro. The conductor was submitted to an effective current of 10.4kA during 0.5 seconds. The temperature in the mid position of the tube wall as well as the temperature in the center of the wire was measured, by using a data acquisition system National Instruments – DAQCard-AI-16XE-50, SCXI (1000, 1120, 1181, 1328 and 1203). In order to correlate the induced vibration of the conductor with the thermal response due to the short-circuit test, a traction measuring cell HBM, model S9 was utilized.

The experimental results are plotted in Figures (7) and (8). The temperature distributions T_i and T_{ao} are calculated by equations (19), (20), (21) and (22), where by definition of θ , $T_i = T_o (1 + \theta_i)$ and $T_a = T_o (1 + \theta_{ao})$. The parameters p_i and p_a were calculated at an equivalent reference temperature T_r . This temperature is determined by comparing the numerical results obtained from the present model with the numerical results obtained from the solution corresponding to the thermal capacitance model (MCT), by considering temperature-dependent electric resistances. The non-linear equations were solved by the Runge-Kutta method. Details are found in [4]. The present solution is plotted in Figure (7) for different values of the parameter B_{ic} .

It is seen in Figure (7) that the best agreement of the present solution with the experimental results is found for B_{ic} around unity. The present model is shown to be able to predict the maximum temperature for $B_{ic} = 1$. However, the results of the present model deviates from the experimental data in the cooling period of the short-circuit test. The solution presented here is a rather simplified one, and therefore is not appropriate to describe completely the heat conduction effects in the OPGW analyzed here. On the other hand, one can conclude that the contact thermal resistance may be affected by the mechanical deformations during the cooling of the conductor. Figure (8) may be helpful to explain the mechanical effects mentioned.

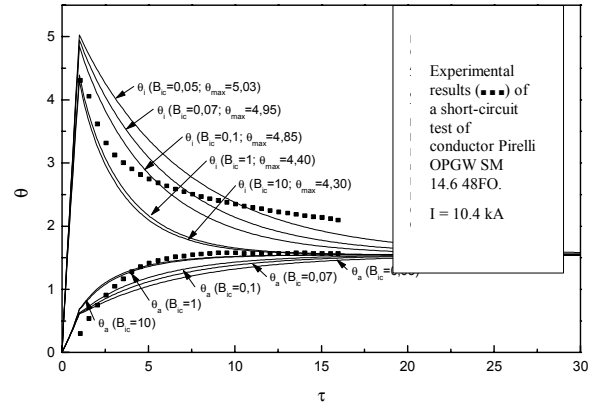


Figure 7. Comparison of predicted results for $T_r = 120^\circ C$ and the experimental results, in terms of the dimensionless temperature of the tube (θ_i) and the dimensionless temperature at the center of the wires (θ_{ao}) as functions of $\tau = t / \Delta t_c$

The large amplitude of the measured traction may be correlated to the relative longitudinal displacement between the wires and the tube. Due to the difference between the coefficients of thermal expansion of the aluminum and the steel, and because of the large temperature difference between the wires and the tube during the cooling period, the contact strips existing in the interface between the wires and the tube may change in size, thus increasing the thermal resistance. Since the present solution does not allow for different values of B_{ic} for the heating and the cooling period, it is not appropriate to investigate the effect of the variation of B_{ic} with time. In order to minimize this limitation, a more general model is presently being developed by the authors. This model takes into account higher order terms of the Galerkin boundary condition given by equation (10), as well as the variation of B_{ic} with time in the cooling period. The model mentioned is believed to be adequate for the parameter estimation of B_{ic} and φ_o .

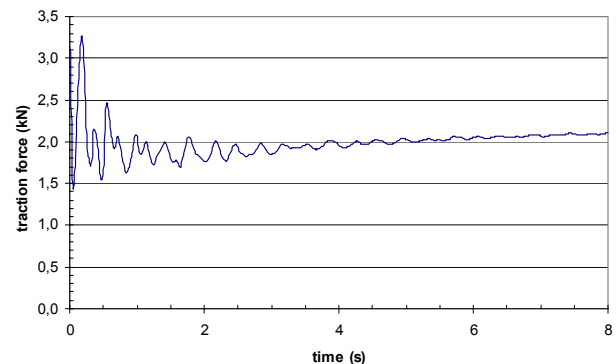


Figure 8. Plot of the traction force measured by the traction cell during the short-circuit test

4. Conclusions

The present paper reported an analytical solution for the temperature distribution of OPGW submitted to a short-circuit current. The results presented here are expressed in terms of dimensionless parameters, which may be of practical interest for the thermal design of OPGW. The predicted temperature distribution agrees with the experimental data for the heating period. However it is in disagreement with the experimental results for the cooling period. Further work is needed in order to characterize the contact thermal resistance between the wires and the conductor tube, in terms of parameters B_{ic} and the effective contact angle φ_o .

5. Acknowledgments

The authors are indebted to the engineering students Mrs. Karime Zenedin Glitz and to Mr. Carlos Eduardo da Veiga, for helping with the computation of the analytical solutions. The authors are also indebted to Eng. Mr. Fábio Vilas Boas Ribeiro, for helping with the data acquisition in the short-circuit tests carried out at CEPTEL.



Prof. Sergio Colle
LABSOLAR / NCTS – Department of Mechanical Engineering
– UFSC (Federal University of Santa Catarina)
88040-900 – Florianópolis – SC – Brazil

Bibliography:

Mechanical Engineer degree in 1970 - UFSC
Master of Science in Mechanical Engineering in 1972 – COPPE / University of Rio de Janeiro
Doctor of Science in Mechanical Engineering in 1976 – COPPE / University of Rio de Janeiro
Professor of Thermodynamics, Heat Transfer and Solar Energy – Department of Mechanical Engineering – UFSC since 1974
Consulting Engineer of PIRELLI in the field of heat transfer and applied thermodynamics
Head of LABSOLAR/NCTS.

6. References

- [1] N. Özisik, “Boundary Value Problems of Heat Conduction,” *Int. Textbook Company*, Scranton, Pennsylvania, (1968).
- [2] V. S. A. Arpaci, “Conduction Heat Transfer,” *Addison Wesley*, (1966).
- [3] I. Stakgold, “Boundary Value Problems of Mathematical Physics – Vol. II,” *Macmillan*, (1968)
- [4] S. Colle, “Technical Reports No. 1-5 to Pirelli Telecommunication Cables and Systems of Brazil,” *Department of Mechanical Engineering, UFSC*, (2002-2003).
- [5] R. S. Madge, S. Barret and H. Grad, “Performance of Optical Wires During Fault Current Tests,” *IEEE Transactions on Power Delivery*, 4 (3), (July, 1989).
- [6] F. Jakl and A. Jakl, “Investigation of Temperature Rise of ACSR Conductors and OPGW under Short – Circuit Conditions,” *CIGREE WG12*, No. 22-96.



Eng. Marcelo de Araújo Andrade
Pirelli Telecomunicações Cabos e Sistemas do Brasil AS
Avenida Pirelli, 1.100 – Éden
18103-355 – Sorocaba – SP – Brazil

Bibliography:

Was born in Florianópolis – SC, Brazil in 1965
He was graduated from Federal University of Santa Catarina
He joined Pirelli in 1988 where he in charge of Telecom Engineering and Quality.